# Production of leaf wax *n*-alkanes across a tropical forest elevation transect

Sarah J. Feakins[a*], Tom Peters[a], Mong Sin Wu[a], Alexander Shenkin[b], Norma Salinas[b,1], Cécile Girardin[b], Lisa P. Bentley[b], Benjamin Blonder[b], Brian J. Enquist[c], Roberta E. Martin[d], Gregory P. Asner[d], Yadvinder Malhi[b]

[a] Department of Earth Sciences, University of Southern California, 3651 Trousdale Pkwy, Los Angeles, CA 90089, USA

[b] Environmental Change Institute, School of Geography and the Environment, University of Oxford, South Parks Road, Oxford, OX1 3QY, UK.

[c] Department of Ecology and Evolutionary Biology, University of Arizona, AZ 85721, USA.

[d] Department of Global Ecology, Carnegie Institution for Science, 260 Panama St, CA 94305, Stanford, USA.

*Submitted to Organic Geochemistry*

*Corresponding author: Sarah J. Feakins, email: feakins@usc.edu, phone: 213 740 7168

[1] Permanent address: Seccion Química, Pontificia Universidad Católica del Peru, Peru.

Author Contribution Statement

S.J.F designed and led the leaf wax study; Y.M. designed and led the CHAMBASA field campaign; Y.M., B.J.E., G.P.A., L.P.B., N.S. and A.S. planned the fieldwork; L.P.B., N.S. and A.S., conducted the fieldwork; R.E.M. led taxonomic classifications; C.D. contributed productivity data. T.P. conducted the leaf wax laboratory work and data analysis and M.S.W. contributed; S.J.F. conducted the data analysis, graphing and wrote the manuscript. All authors contributed to discussions.

**Abstract**: Waxy molecules form the boundary layer of the living leaf and contribute molecular fossils to soils, lake and marine sediments. Cataloguing the variations in leaf wax traits between species and across environmental gradients may contribute to the understanding of plant functional processes in modern ecosystems, as well as to the calibration efforts supporting reconstructions of past ecosystems and environments from the sedimentary archives of leaf wax biomarkers. Towards these goals, we survey leaf wax *n*-alkanes in trees from the lowland tropical rainforest (TR) and montane cloud forest (TMCF) of Peru. Leaf wax molecular abundances were quantified via gas chromatography flame ionization detection (GC-FID) for 635 individuals, 152 species, 99 genera and 51 families across 9 forest plots spanning 0.2–3.6 km elevation. We find the expected molecular abundances distributions, for example the *n*-alkane component of plant leaf waxes is dominated by long chain, odd numbered *n*-alkanes, especially $C_{29}$ and $C_{31}$. New observations include a tendency to increasing total alkane concentrations at higher elevations. We propose that the well-known leaf economic strategy to increase leaf mass per unit area with elevation, yields a theoretical basis for understanding the observed increase in leaf wax *n*-alkane abundance with elevation: we infer an increased investment in foliar defense in response to environmental pressures thought to include cloud immersion and declining temperature. Furthermore, we combine measurements of *n*-alkane concentration with estimates of forest productivity to provide new ways to quantify ecosystem-scale forest alkane productivity. We introduce a new concept of *n*-alkane net primary productivity ($NPP_{alk}$; the product of alkane concentration and leaf NPP) and find that alkane productivity estimates ranges from 300–5000 g C $ha^{-1}$ $yr^{-1}$ associated with ecological and environmental changes across the elevation profile.

**Keywords**: Amazon; Andes; CHAMBASA; leaf wax; Peru; NPP

## 1. Introduction

Terrestrial plants leaves are covered with waxes, comprised of mixtures of long-chain hydrocarbons, including *n*-alkanes, *n*-alkanols, aldehydes, fatty acids, and wax esters, with the *n*-alkanes commonly dominating the mixture (Eglinton & Hamilton, 1967). Wax components are synthesized early in leaf ontogeny (Jetter and Schaffer, 2001) and likely not substantively regenerated during the lifespan of the leaf (Kahmen et al., 2013a; Tipple et al., 2013), although replacement following erosion of surface waxes has been demonstrated (Jetter and Schaffer, 2001). The epicuticular and intracuticular waxes on plant leaves serve to protect the plant from desiccation, from pathogen and fungal attack, as well as altering leaf wettability and runoff (Koch et al., 2009). This protective role may extend to other functions, including protection from UV radiation (Shepherd & Griffiths, 2006). Many of these functions of leaf waxes would be expected to vary across elevation gradients, which carry environmental gradients in temperature, precipitation, insolation and biotic stressors.

The molecular abundance distribution of leaf waxes varies between species (Diefendorf et al., 2011). Of the long chain *n*-alkanes, with the molecular formula $C_nH_{2n+2}$, where n typically is 21 to 35, typically one or two chain lengths are dominant or co-dominant and distributions have a strong odd-over-even preference resulting from chain elongation by acetate units followed by decarboxylation (Eglinton and Hamilton, 1967). Discrete applications where *n*-alkane distributions are diagnostic may be the exception rather than the rule, for example, *Sphagnum* in peat bogs dominantly make $C_{23}$ (Bingham et al., 2010), whereas *Juniperus virginiana* dominantly makes $C_{35}$ (Tipple and Pagani, 2013) but these are rarely dominant in other species. Some studies have suggested that chain length distributions of *n*-alkanes can discern shifts in

71 vegetation communities such as forest-grassland transitions in the high Andes (Jansen et al.,
72 2010) or grassland-succulent plant transitions in southern Africa (Carr et al., 2010). Variations in
73 molecular abundance distributions have also been suggested to be responses to temperature or
74 aridity at the time of leaf production in *J. virginiana* (Tipple and Pagani, 2013) or aridity in
75 *Acacia* and *Eucalyptus* (Hoffmann et al., 2013). Studies of atmospheric dust (Kawamura et al.,
76 2003) and marine sediments (Castaneda et al., 2009) provide supporting evidence for these
77 suggested relationships between chain length and temperature or aridity. However, the variety of
78 molecular distributions between species appears to confound the search for globally consistent
79 environmental responses in leaf wax molecular abundance distributions (Bush and McInerney,
80 2013). A diversity of molecular abundance distributions might therefore be expected to be
81 greatest in regions of high phylogenetic diversity (Ter Steege et al., 2010) and functional
82 diversity (Silman, 2014), such as biodiverse tropical rainforests.

83 **1.1. Tropical plant leaf wax studies**

84 Very little direct work on living plants has been done to date in lowland tropical ecosystems in
85 terms of characterizing leaf wax composition (Vogts et al., 2009; Garcin et al., 2014; Graham et
86 al., 2014). Those studies focused on carbon isotopic variations as well as molecular abundance
87 distributions of a few species in central Africa and central America. Across a forest-grassland
88 transition in Cameroon the varying proportions of wax production in different chain lengths were
89 shown to impact the overall isotopic signature contributed to sediments, with the $C_4$ grass types
90 contributing $C_{33}$ *n*-alkanes, whereas $C_3$ trees and shrubs dominating the $C_{29}$ and $C_{31}$ *n*-alkanes
91 (Garcin et al., 2014). Whether the varied concentration of waxes on the leaves of different
92 species may bias the sedimentary signal is an important question to investigate further.

93 In the Andes, plant leaf waxes have been studied in living plants in the tropical montane forests
94 and *páramo* (alpine tundra, mostly grasses) in the Ecuadorian Andes (Jansen et al., 2006). In
95 almost all plants sampled, the $C_{29}$ and $C_{31}$ were found to be the dominant *n*-alkanes with the
96 expected odd over even chain length preference (Jansen et al., 2006; Jansen and Nierop, 2009).
97 The ratio of $C_{29}$:$C_{31}$ *n*-alkanes has been suggested as an indicator of the forest-*páramo* transition
98 in the Ecuadorian Andes, with paleoenvironmental reconstructions using this as well as other
99 aspects of molecular abundance distribution and pollen (Jansen et al., 2010; Jansen et al., 2013).
100 The absolute concentrations have been found to vary greatly between species and plant types
101 with concentrations of the $C_{29}$ *n*-alkane ranging between negligible and up to 1600 μg $g^{-1}$.
102 However, in those Andean studies, plant sampling extended no lower than 3.5 km, leaving the
103 western Amazon unstudied.

104 **1.2. Elevation transect**

105 The western Amazon contains some of the highest plant species diversity in the world (Ter
106 Steege et al., 2010). This high biodiversity adjacent to the Andes may not be unrelated: the uplift
107 of the Andes dramatically altered landscape and climate, and may have contributed to species
108 diversification (Hoorn et al., 2010). The Eastern Cordilleran uplift began with the "Incaic pulse"
109 of uplift of the central Peruvian Andes during the Eocene and this phase of uplift was complete
110 by 40 Ma (Noble et al., 1979). A fully-forested elevation transect across the eastern flank of the
111 Andes has been sampled by a series of plots that allow, amongst other things, the study of tree
112 species diversity (Silman, 2011), forest productivity (Girardin et al., 2014a; Huacara Huasco et
113 al., 2014; Malhi et al., 2014), and the effects of environmental variables on plant traits (Malhi et
114 al., 2010; Asner et al., 2014a; Asner et al., 2014b; Girardin et al., 2014b). This transect of forest
115 plots has recently been used to study plant water and leaf wax hydrogen isotopic compositions,

with plants found to encode the isotopic composition of meteoric water in the leaf wax *n*-alkane and *n*-alkanoic acids (Feakins et al., 2016).

From this same network of forest plots, we analyze a large set of leaf samples, in total sampling 639 individual trees of which 158 species from nine sites, greatly expanding the available catalogue of leaf wax *n*-alkane abundance information on tropical trees. This study yields new insights into the patterns of individual and community *n*-alkane abundance and molecular composition to reveal landscape and ecosystem-scale assessments of tropical forest leaf wax *n*-alkane production.

### 1.3. Geological relevance

These leaf wax *n*-alkanes are of geological interest as they are notably resilient tracers of past plant production. Leaf waxes, abraded by wind, water or insects, or carried on senescent leaves into leaf litter and soils, may be stored, or eroded and transported further to lake and ocean sediments (Hemingway et al., 2016). In the high Ecuadorian Andes (>3.5 km), *n*-alkane storage times in soils has been estimated to span several millennia (Jansen and Nierop, 2009). Some fraction of those leaf waxes may be remineralized by microbial activity, but the waxes are the more recalcitrant of the many biochemicals produced by plants and thus their proportion in sedimentary organic matter increases as other more labile compounds such as carbohydrates and cellulose degrade (Hedges and Oades, 1997). Of the leaf waxes, *n*-alkanes are commonly used in palaeoenvironmental studies, including records that extend back over at least 55 Ma into the hyperthermal conditions of the Paleocene-Eocene Thermal Maximum (Pagani et al., 2006; Handley et al., 2012; Krishnan et al., 2015). Plant leaf waxes may therefore have the potential to inform on the long-term evolution of the Amazon rainforest (Hoorn et al., 2010), in suitable sedimentary archives.

Leaf waxes have been studied in soils, as well as in fluvial sediments exported by the Kosñipata and Madre de Dios rivers draining the eastern flank of the Andes down to the Amazonian lowlands, with their hydrogen isotopic composition tracing their elevation or origin and downstream integration across the catchment and informing on modern transport and storage processes (Ponton *et al.*, 2014). Elsewhere the molecular abundance distributions of leaf waxes have been studied in soils to reconstruct the forest-*páramo* transition at high elevation in the Ecuadorian Andes over millennia (Jansen et al., 2010; Jansen et al., 2013). The same molecules have been studied in the surface sediments of lakes, and their hydrogen isotopic compositions used to discern spatial variations in aridity (Polissar and Freeman, 2010). Hydrogen isotopic compositions have been used to reconstruct past changes in hydroclimate across the last glacial and the Holocene with a record spanning 12,000 years from Lake Titicaca, Peru/Bolivia (Fornace et al., 2014), as well as in a smaller lake setting, where ecological changes in the vegetation community superseded the hydroclimate signal (Fornace et al., 2016). Prior marine sediment reconstructions using leaf waxes around South America include reconstructions for the late Pleistocene from the Cariaco Basin off Venezuela (Hughen et al., 2004). As leaf waxes may be preserved in the geological deposits for millions of years (Hedges & Oades, 1997) there is potential for future work on Neogene and older leaf waxes within continental drilling in the Amazon basin (Baker et al., 2015) and for reconstruction from marine sediments of the Amazon Fan as well. The goal of better understand the significance of the leaf wax legacy of ancient ecosystems in tropical paleoenvironmental sedimentary records motivates studies of living forests across environmental gradients.

## 2. Materials and Methods

### 2.1. Study site

This study included 9 plots (Fig. 1; Table 1) that belong to a group of permanent 1-ha plots operated by the Andes Biodiversity Ecosystems Research Group (ABERG, http://www.andesconservation.org) and that are part of the ForestPlots (https://www.forestplots.net/) and Global Ecosystems Monitoring Network (GEM; http://gem.tropicalforests.ox.ac.uk/projects/aberg) networks. Five montane plots are located in the Kosñipata Valley in the province of Paucartambo, in the department of Cusco, Peru, two are sub-montane plots located in the Pantiacolla front range of the Andes and two lowland plots are located in Tambopata, in the department of Madre de Dios, Peru (Malhi et al. 2010). All plots are located in areas that have relatively homogeneous soil substrates and stand structure, and which have minimal evidence of human disturbance (Girardin *et al.* 2014a). The sites are placed to sample across the profile, and to characterize the full range of forest and climate. The highest site is located just below the treeline transition to *puna* (grassland); two sites bracket the cloud-base and two lowland sites test influence of proximity to the river (Fig 1). The lowland plots were established in the early 1980s, and the montane ones between 2003 and 2013, with all stems ≥10 cm diameter at breast height tagged and identified to species-level, and plots have been annually measured for carbon allocation and cycling following standard the GEM Network protocol (Marthews *et al.*, 2014). As such, net primary productivity estimates (Girardin *et al.* 2010) and comprehensive descriptions of the carbon cycle exist for many of these plots (Girardin *et al.* 2014b; Huaraca Huasco *et al.*, 2014; Malhi *et al.*, 2014; Malhi *et al.*, 2015). Mean annual air temperature spans 9–24.4°C and precipitation spans 1560–5302 mm $y^{-1}$ along the gradient (Table 1).

### 2.2. Field sampling

From April – November 2013, plant traits were measured in all plots as part of the CHAMBASA project. Based on the most recently available census and diameter data, a sampling protocol was adopted wherein species were sampled that maximally contributed to plot basal area (a proxy for plot biomass or crown area). Within each species, 3–5 individual trees were chosen for sampling (5 trees in upland sites and 3 trees in lowland sites). If 3 trees were not available in the chosen plot, additional individuals of the same species from an area immediately surrounding the plot were sampled. Using advanced tree climbing techniques, leaves samples from one fully, sunlit canopy branch (of at least 1 cm diameter), were taken from each tree. Some companion shade leaves were selected for other projects. From each branch, measurements were taken of 5 leaves from simple-leaved species, or 5 individual leaflets from compound-leaved species (both referred to as 'leaf' below) for trait measurements. In the case of compound leaves, the entire compound leaf was also collected for whole-leaf area calculations. Leaves were chosen with minimal damage (i.e. herbivory). Leaves were placed in coolers from the field plot to the field lab for drying, at low temperatures (ca. 50 °C), and thereafter stored in paper envelopes prior to lipid analysis. The sample set for *n*-alkane quantification includes 639 individual samples distributed across 9 forest plots, including 158 species from 105 genera and 55 families.

### 2.3. Lipid extraction

The dried leaves were cut using solvent-cleaned scissors and leaf waxes were subsequently extracted by immersion in dichloromethane (DCM)/methanol (MeOH) 9:1 v/v with agitation using a Pasteur pipette, with extraction repeated x3. The total lipid extract was separated into two fractions using column chromatography (5 cm x 4 mm Pasteur pipette, 5% water-deactivated silica gel, 100-200 mesh), eluting first with hexane (alkanes fraction), followed by DCM, and MeOH (remainder). Only the alkane fraction was analyzed here.

### 2.4. *n*-Alkane identification and quantification

The alkane fraction was analyzed by an Agilent Technologies® gas chromatograph connected to a mass spectrometer and flame ionization detector (GC-FID/MS) to identify (by MS) and quantify (by FID) the *n*-alkanes. Peak areas by FID were manually integrated to quantify *n*-alkanes in the range of $C_{21}$ to $C_{35}$ carbon chain length, relative to daily analysis of the external standard and in-house mixture of *n*-alkanes of known abundance. We report the abundances for each chain length and also report the modal chain length ($C_{max}$). We calculate the average chain length (ACL), which is the weighted average accounting for concentration ($C_n$) of each compound (n) computed as:

$$ACL = \Sigma (C_n \times n) / \Sigma C_n \quad (1)$$

where n = 27 to 33.

The *n*-alkanes were summed as:

$$\Sigma alk = \Sigma_i^n [C_n] \quad (2)$$

where n = *n*-alkanes from $C_{21}$ to $C_{35}$. This sum of *n*-alkanes can be considered as concentration relative to per unit dry leaf mass reported in units of $\mu g\ g^{-1}$ or per unit leaf lamina area reported in units of $\mu g\ cm^{-2}$. In order to consider the C fixation, alkane concentration can be converted from units of $\mu g\ g^{-1}$ (dry leaf tissue) into $\mu g\ g^{-1}$ C, by accounting for the molar fractions of C in both alkanes and dry bulk leaf tissue. The molar fraction of C is 0.8529 for the $C_{29}$ *n*-alkane, the dominant chain length and within error the result is insensitive to the choice of chain length, making it unnecessary to account for variations in molecular distribution. For leaf biomass (~50% C), we used the measured C content of leaf biomass on a per species basis. Each of these ways of evaluating the alkane concentration is used for calculations and comparisons here.

We calculated the Carbon Preference Index (CPI) as:

$$CPI = 2\,\Sigma C_n / \Sigma C_{n-1} + \Sigma C_{n-1} \quad (3)$$

where n = 27-33. For comparison purposes, we also calculated the ratio of two common chain lengths, $C_{29}/C_{31}$, as this index has been reported elsewhere in the Andes (Jansen and Nierop, 2009).

### 2.5. Community averages

We analyzed the distribution of leaf wax traits for individuals and calculated medians and unweighted means of all sampled individuals at each forest plot. Means are influenced by outliers and this results in biased central estimates when data distributions are highly skewed, where medians are more appropriate measures of the central tendency. The numbers of individuals and species sampled, as well as the proportion of the forest represented by the sampled species, inform on the representation achieved by our sampling.

Leaf wax traits for individuals were also averaged at the species level within each forest plot, and we computed weighted-means that account for the proportional contribution of each species, based on estimates of biomass. To estimate biomass, we used tree trunk diameter at breast height from the year with the most recent census data. While census year ranges between 2009 to 2014, it is not expected to bias analyses since plots are old growth and have not experienced major disturbance (e.g. landslide, fire, deforestation) during that time. We weight on the basis of the total basal area of each sampled species within the forest plot. For ACL, CPI and 29/31, the community-weighting accounts for variations in both species' basal area and alkane concentrations. The weighted means (cwm) and the weighted standard deviations ($\sigma_w$) for each trait at the plot level were estimated using:

$$cwm = \Sigma C_i^n \, w_i \, x \, x_i \, / \, \Sigma C_i^n \, w_i \quad (4)$$

$$\sigma_w = \sqrt{} \, (\Sigma_i^n \, (w_i \, x \, cwm)^2 \, / \, \Sigma_i^n \, w_i \,) \quad (5)$$

where $x_i$ is the value and $w_i$ is the weight for the $i^{th}$ species. Means and standard deviations throughout are estimated from the sample set and not determined for the full population, but the $\sigma$ symbol is used in keeping with convention in the organic geochemical literature. Note that this species weighting approach accounts for interspecies variations and contributions, but does not propagate intraspecific variations (working shown in **Appendix A**).

We report the median, unweighted and community-weighted means for each forest plot to identify the central tendency and the uncertainties on our estimates, as each approach carries known and unknown inaccuracies. For example, medians and unweighted means do not account for biomass, however weighted means and unweighted means of small numbers of samples carry the unquantified uncertainty of small samples of the species they average, particularly where distributions are skewed. The comparison between central estimates thus provides a more comprehensive measure of uncertainties than provided by the standard errors of the mean.

### 2.6. Alkane productivity at the plot-level

Average production of alkanes as a fraction of leaf biomass on a stoichiometric basis can be connected with $NPP_{leaf}$ estimates for each plot (Girardin *et al.*, 2014a; Huaraca Huasco *et al.*, 2014; Malhi *et al.*, 2014) to generate estimates of the Net Primary Productivity of leaf wax *n*-alkanes ($NPP_{alk}$), a term newly coined here, where:

$$NPP_{alk} = \Sigma alk \, x \, NPP_{leaf} \quad (6)$$

Where Σalk refers to the *n*-alkane concentration per site in μg $g^{-1}$ C (variously using the median, unweighted mean of individuals or community-weighted mean of species), and $NPP_{leaf}$ is the leaf net primary productivity in Mg C $ha^{-1}$ $yr^{-1}$. $NPP_{alk}$ is determined for each site and reported in units of g C $ha^{-1}$ $yr^{-1}$ with propagated uncertainties. We report the numbers of samples and species collected as well as the proportion of forest community represented by those species, to describe how much of the forest has been characterized as well as the limits of that sampling that contribute to uncertainty.

## 3. Results

### 3.1. Molecular abundance distribution of *n*-alkanes

We found *n*-alkanes in the range of $C_{21}$ to $C_{35}$, and the abundance of those homologs was determined for 552 individual tree samples, species averages and site averages (Appendix A), revealing considerable variability in molecular abundance distributions. To illustrate average molecular abundance distributions, we summarize the mean of the relative molecular abundance distributions of all individuals 552 individuals (**Fig. 2**). $C_{29}$ and $C_{31}$ are the dominant homologs across all sites with abundances ranging from 20 to 430 μg $g^{-1}$ (*n*-alkane homolog abundance per unit mass of dry leaf). $C_{27}$ alkanes are present at low abundances at the lowland sites, but are more abundant at higher elevations, albeit with lower maxima than $C_{29}$ and $C_{31}$. Most other odd chain length *n*-alkane homologs (i.e. $C_{21}$ to $C_{25}$, and $C_{33}$ to $C_{35}$) and all even chain length homologs are of low abundance throughout (< 30 μg $g^{-1}$).

The putative Andean forest marker, that of $C_{29}/C_{31}$ ranges from <1 up to 128 (**Fig. 3a**), with most individuals having ratios <10, and high ratios found in just a few species: *Weinmannia bangii, Hedyosmum goudotianum and H. cuatrecazanum*. We also report the widely used CPI metric,

293 often used in sedimentary applications as a test of plant source (CPI > 4) versus an indicator of
294 diagenesis (CPI < 4). In this large tropical forest survey, we find CPI to be highly variable
295 between individuals and species ranging between 1 and 53, with an overall mean of 31 ($\sigma$ = 9,
296 range 1-53, n = 552; **Fig 3b**). Notably, 80 individual plants, or 15% of the tropical trees sampled,
297 yield CPI < 4.

298 3.1.1. Data not included in our survey

299 Of the 639 measured samples, 54 individuals were excluded from further calculations, because
300 of chromatographic issues, typically, the non-determination of even chain *n*-alkanes. In those
301 samples where even chain *n*-alkanes could not be identified or quantified, this was due to the
302 presence of other compounds, suspected to be esters at the same point in the chromatogram. An
303 additional 29 samples are reported as additional data that were collected outside of the
304 CHAMBASA tree canopy survey, mostly understory collections at cloud forest site ESP-01, as
305 well as some lianas (vine-like growth forms). These additional data (82 individuals) are reported
306 separately in Appendix A, but are not analyzed further as part of the canopy survey effort here.

307 **3.2. Average Chain Length**

308 The 'fingerprint' of molecular abundance distribution (**Fig. 1**) is commonly summarized by the
309 average chain length (ACL). ACL is highly variable ranging from 27.2 to 32.6 overall (**Fig. 4**),
310 with up to 2 to 5 units of range between individuals at any site. Interspecies variability appears to
311 capture much of this range, although the range of intraspecies variability and small number of
312 samples of each species means that the species mean values are not well-defined. The
313 unweighted mean ACL of all individuals at each site displays a one-unit tendency to longer chain
314 lengths at the lower elevations. Linear regression of ACL data with site mean annual air

315 temperature (MAAT) yields ACL = 0.07 · MAAT + 28 (for individual data $r^2 = 0.19$; $p < 0.05$;
316 for site mean values $r^2 = 0.90$; $p < 0.05$).

317 **3.3. Alkane concentrations**

318 Alkane concentrations (Σalk) varies from 1 to 5225 μg $g^{-1}$ dry leaf mass (**Fig. 5a**). For clarity,
319 we emphasize that wax is a very small component of the leaf, accounting for just 1.12% ($1\sigma$ =
320 0.05%, *n* = 552) on average, from a minimum of 0.0001% to no higher than 5.2% on a leaf mass
321 basis. On a stoichiometric basis, Σalk ranges from 2 to 9766 μg $g^{-1}$ C (**Fig. 5b**). While leaf wax
322 concentration data are commonly reported in concentration units as above, leaf waxes are not
323 dispersed through the leaf but deposited as a layer on the leaf surface, and as with other surficial
324 leaf traits, may be better considered on an area basis. Here, individual Σalk values spans a range
325 of 0.01 to 81 μg $cm^{-2}$ on a leaf area basis (**Fig. 5c**).

326 The alkane concentrations of individual data are highly skewed, and the distributions of
327 individual data and central estimates are displayed in violin plots (**Fig. 6**). Intraspecies variability
328 is high and thus species mean values are not well-determined from small sample sizes (3-5
329 individuals of a species). Examples of species with high alkane concentrations per unit area
330 include *Clethra cuneata* (Clethraceae) and *Myrsine coriaceae* (Primulaceae), and examples of
331 the many species with low concentrations include *Guatteria glauca* (Annonaceae) and *Elaeagia*
332 *mariae* (Rubiaceae). Despite the variability in alkane concentrations between individuals, a
333 significant transition occurs between the TR (lower alkane concentrations) and TMCF (higher
334 alkane concentrations) between 1.5 and 1.7 km (**Fig. 6b**; with mean values being significantly
335 different by Student's t test), corresponding to the transition from sub-montane forest to Tropical
336 Montane Cloud Forest. Above 1.7 km, maximum values for a few individuals and mean values

337 remain high, but distributions and median values reveal that Σalk of most individuals drop in the
338 highest elevations again (**Fig. 6b**). But, pulled by the high Σalk of some individuals of dominant
339 species, community-weighted mean values increase further with elevation. We therefore observe
340 a divergence between total alkane concentration estimates from forest plots central estimates
341 with elevation within the TMCF median (decreasing), mean (plateau) and community weighted
342 mean (increase) (**Fig. 7b**). For skewed data distributions the median is advised, however as
343 trends are dependent upon statistical choices, at the highest sites, particularly ACJ-01,
344 uncertainties are revealed by the comparison between central estimates.

345 **3.4. Forest plot alkane productivity**

346 In order to assess productivity, we combine observations that *n*-alkane concentrations tend to
347 increase across the profile (**Fig. 8a**), with observations that $NPP_{leaf}$ decreases with elevation
348 (Girardin *et al.*, 2014a; Huaraca Huasco *et al.*, 2014; Malhi *et al.*, 2014; Table 2, **Fig. 8b**). The
349 product of these two measures, by Eqn. 6, yields $NPP_{alk}$ estimates (**Fig. 8c**). $NPP_{alk}$ plot-level
350 ranges from 321 to 3029 g $ha^{-1}$ $yr^{-1}$ based on median alkane concentrations; 552 to 3394 g $ha^{-1}$
351 $yr^{-1}$ based on the unweighted mean alkane concentrations and 595 to 5123 g $ha^{-1}$ $yr^{-1}$, using the
352 community-weighted approach. For the lowland tropical rainforest, distal from the river (TAM-
353 05) we estimate $NPP_{alk}$ to be 1098-1513 g $ha^{-1}$ $yr^{-1}$ depending on estimation method, we see
354 lower productivity closer to the river (TAM-06; 686-1199 g $ha^{-1}$ $yr^{-1}$). From low alkane
355 productivity in sub-montane forests at 0.6 km (PAN-02; 340-944 g $ha^{-1}$ $yr^{-1}$), we find a robust
356 increase in $NPP_{alk}$ with elevation to 2.7km (TRU-04; 2553-3394 g $ha^{-1}$ $yr^{-1}$). TMCF plots (3
357 sites) between 1.7 and 2.7 km have notably higher alkane production rates at approximately
358 double or triple those of the lowland and sub-montane plots (**Fig. 8c**), and this corresponds to an

359 increase in the proportion of $NPP_{leaf}$ diverted to alkane production from 0.02% to 0.13% across
360 the profile.

361 We find divergent estimates for the upper plot (ACJ-01) depending on statistical methods
362 chosen. The median provides the lower bound estimate and indicates a low productivity at the
363 highest site (513 g $ha^{-1}$ $yr^{-1}$), which is similar to that of the low productivity sites in the sub-
364 montane forests. While some species, including the co-dominant species (*Clethra cuneata and*
365 *Weinmannia fagaroides*), have high alkane concentrations, those concentrations are variable
366 between individuals, thus the weighted standard error likely underestimates uncertainty. We
367 therefore find that our estimates at the highest site, are not robust to statistical choices and we
368 present the range of estimates for this plot, as a measure of uncertainty here.

369 **4. Discussion**

370 **4.1. Molecular abundance distribution of *n*-alkanes**

371 From our tropical tree dataset, we can analyze the patterns of leaf wax *n*-alkane molecular
372 distributions. In any one species, individual odd chain length *n*-alkanes in the range $C_{21}$ to $C_{35}$
373 may be dominant and distributions vary between species and with species turnover across the
374 transect. The implications are that not all chain lengths can be followed across an environmental
375 gradient and no *n*-alkane is a unique 'marker' for a species. The mean molecular abundance
376 distribution (**Fig. 2**) shows two *n*-alkanes dominate overall: $C_{29}$ and $C_{31}$. These cosmopolitan
377 molecules may serve as biomarkers in widespread sedimentary applications, whereas other
378 molecules have more limited sources. $C_{29}$ and $C_{31}$ dominance have been observed in other
379 studies of $C_3$ trees in the rainforests of Cameroon, Africa (Garcin et al., 2014), but this is the first
380 such demonstration from so many species at the warm and wet extremes of global calibration
381 efforts (Sachse et al., 2012) and from the rainforests of Peru. In sedimentary archives, $C_{29}$ and

382 $C_{31}$ are common analytical targets because of their abundance. For example, $C_{31}$ was the
383 dominant homolog in marine sediments of Site 1077 receiving input from the Congo rainforest,
384 Africa and the target for $C_3$ versus $C_4$ vegetation reconstructions (Schefuss et al., 2003), and $C_{29}$
385 was the dominant homolog in marine sediments of GeoB 6519-1 used for paleohydrological
386 reconstructions using hydrogen isotopic composition (Schefuss et al., 2005). Our study of
387 Peruvian trees would suggest that both these chain lengths are characteristic of tropical trees. In
388 contrast, the $^{13}$C-enriched contributions from $C_4$ grasses may be better detected in the $C_{33}$ and $C_{35}$
389 *n*-alkanes, which have been found to be more abundant in African grasses (Garcin et al., 2014).

390 While $C_{29}/C_{31}$ has been suggested as an Andean forest marker (Jansen et al., 2008), separating
391 high elevation grasslands (<1) from Andean forests (>1) in that study in Ecuador. Here, we find
392 that high values (>10) in a few tree species *Weinmannia bangii, Hedyosmum goudotianum and*
393 *H. cuatrecazanum*, whereas most tree species, have ratios <10. Overall site median values range
394 from 0.9 to 3.3 in this forested transect, with values <1 in so many species (especially lowland
395 tree species) that we suggest chain length distributions may not be a secure marker for forest-
396 grassland transitions without additional evidence from pollen (Jansen et al., 2013).

397 In sedimentary applications, CPI is often considered when evaluating plant source, and here we
398 find the expected odd-over-even chain length preference. But, we note that CPI<4 are found in
399 80 individual plants, or 15% of the tropical trees sampled, and thus the use of CPI to diagnose
400 plant sources versus diagenesis or petrogenic sources should acknowledge the diversity of
401 molecular distributions seen in living (tropical) plants. In particular the low CPI in 15% of trees
402 in this study, would suggest caution or further quantification of these effects might be
403 appropriate in mixing model deconvolution efforts separating plant and petrogenic sources
404 (Pearson and Eglinton, 2000).

### 4.2. Average Chain Length

The average chain length (ACL) of *n*-alkanes tends to increase towards lower elevations (**Fig. 3a,b**) and this has been hypothesized to be due to higher temperatures. However, the overall 15.4 °C temperature increase across 3.3 km results in only a one carbon chain length increase in site mean ACL. We also note substantial variability between individuals (**Fig. 3a**). While the central tendency of ACL is to decrease with elevation (**Fig. 3**), the low temperature sensitivity and high taxonomic variability (**Fig. 3a**) leads us to discount ACL as a proxy for temperature, at least in these TR and TMCF ecosystems, consistent with the conclusions of Bush & McInerney (2015). The response to temperature is not sensitive enough to be compelling for application to paleoenvironmental reconstruction, given the two-to-five times larger variance of ACL within a site, thus ACL is not discussed further here.

### 4.3. Higher *n*-alkane concentrations on plant leaves with elevation

Our results show that some tree species in the upper elevation TMCF produce more *n*-alkanes than tree species in the sub-montane zones, with a clear increase between 0.6 and 2.7 km. This increase in alkane concentration likely confers certain benefits to the leaf for defense and structure. Although herbivory is a major pressure in tropical forests, herbivory decreases with elevation (Metcalfe et al., 2014) and is therefore unlikely to explain the increase in Σalk with elevation in the montane zone, but may explain the greater alkane concentrations in the lowland than the sub-montane zone. We note an increase in mean and median *n*-alkane concentrations (**Fig. 5a, b**) between SPD-02 and SPD-01 bracketing the cloud base ca. 1.5 km (Halladay *et al.*, 2012a). We hypothesize that frequent fog immersion promotes epiphyll growth, and wax provides a barrier to ephiphylls, fungi and other pathogens (Koch et al., 2009). Both sites are in a very wet climatic zone with c. 5 m MAP, and the need to shed precipitation and provide

structural support is unlikely to differ substantially between the two sites. The waxy layer on the upper surface of the leaf adds to thickness, also provides protection against freezing temperatures at night at high altitude (Beck, 1994). The maximum Σalk of some individuals and species continue to rise at higher elevations, although median values drop at the highest site (ACJ-01 at 3537 m), after accounting for dominance the community-weighted mean increases. While waxes may also be involved in shielding against UV-B radiation at these highest altitude, where cloud cover and atmosphere thins, we do not find robust evidence for this response (**Fig. 5d**). While *n*-alkane concentrations may have multiple selective pressures, in this elevation transect, we find the main difference to be between the lowland rainforest and the wet cloud immersion zone and maximum in precipitation amounts within the TMCF and thus infer that the wet zone is the dominant causes of high *n*-alkane concentrations.

### 4.4. Leaf wax trait diversity in the context of species diversity

Given the high beta diversity (Condit et al., 2002), site-to-site variations in leaf wax traits are accompanied by species replacement. Hence changes in plot-level waxiness are more likely related to species (as well as genus and family) turnover of a phylogenetically conservative trait (Eglinton et al., 1962; Eglinton and Hamilton, 1963), rather than through intra-specific plasticity. While this question cannot be resolved here (without transplanting species for example), this study offers insights from the few species present at more than one site. Out of only 23 species found at more than 1 site, most occur within sites <300 m elevation, a narrow environmental range. Of those species, 11 show decreasing ACL values and 6 show increases in leaf wax concentration with elevation, and only 2 species (i.e. *Caryocar pallidum*, *Clusia elliptica*) show both. Our findings are consistent with the hypothesis that long-term evolutionary responses dominate the selection of leaf wax traits across the environmental gradient, rather than recent

451 selective filtering in response to environment. A particularly strong driver appears to be long-
452 term adaptation to cloud forest or extreme high elevation environments by plant families with
453 waxy leaves. Controlled experiments in the laboratory, or translocation experiments along the
454 elevation profile, could directly test whether leaf wax traits can adjust to the rapid environmental
455 change, or if they are fixed by their taxonomy with slower evolutionary responses.

456 **4.5. Community-weighted averaging of leaf wax traits**

457 Sampling was guided by census data such that sample distribution and the unweighted median
458 and mean of that sample set may be representative of the forest plot population. In the diverse
459 lowland forest plots (<1 km) our sampling of species included species representing 18–49% of
460 plot basal area whereas at upland sites >1000 m the greater dominance meant that we achieved
461 higher rates of representation with 36–73% of species basal area sampled (**Fig. 5, Appendix A**).

462 We further calculate species means and account for the biomass and dominance of those species
463 to achieve community-weighted means. This approach is designed to achieve proportional
464 representation of species-means, however small samples of each species, and high interspecies
465 variability, particularly for a trait with skewed distributions, means that high values can bias both
466 species and plot-means. While we report the community-weighted mean estimate, we find the
467 unweighted median to be the more appropriate choice given the skewness of this plant trait,
468 although the community-weighted mean to be the approach of choice for other traits, such as
469 isotopic compositions of these leaf waxes, that have less skewed distributions (e.g., Feakins et
470 al., 2016).

471 Given large sample sizes of individuals, unweighted central estimates may provide a robust
472 approximation of the central value of the forest plot population (Paine et al., 2015). Community-

weighting schemes may better account for the dominance of tree species, particularly in upper TMCF locations where species dominance increases (e.g. *Weinmannia* species), however these species-based weighting schemes are subject to uncertainties introduced by large intraspecific variations in traits. Given the higher intraspecies variability and small samples (typically 3–5 individuals of each species), under-sampling of within species variability contributes unquantifiable uncertainty to the community-weighted mean. Comparisons between methods provides a measure of that uncertainty. We find that community-weighting has the largest impact on *n*-alkane concentration at the highest site in the TMCF (**Fig. 4c, d**), where some of the waxier leaves are found, and where fewer species have greater dominance. At this location the community-weighted mean is double that of the unweighted mean, and is many times greater than the median (**Fig. 8b**). With community-representation we find a strong linear increase in on *n*-alkane concentration with elevation, whereas for the unweighted mean, values plateau, or even decrease for the median at the highest site, leaving our estimates highly divergent and uncertain at this altitude (3.7 km).

### 4.6. A concerted foliar strategy

The increase in *n*-alkane concentrations with elevation can also be considered as part of the overall foliar investment strategy. Increases in LMA with elevation have been linked to the monotonic decline in temperature with elevation as well as limiting nutrients (Poorter *et al.*, 2009) and particularly Ca (Asner and Martin, 2016), which may inhibit growth and canopy stature and lead plants to redirect resources into leaves. The benefits of adding to leaf thickness, in addition to the specific protective roles of wax for leaves, could explain why *n*-alkane concentrations increase more steeply (x5) across the profile than LMA (x1.2 to 1.6) (**Fig. 7a**). Thus alkane concentrations appear to be a sensitive ecological recorder of this environmental

gradient. We hypothesize that increased leaf wax concentrations and LMA have shared roots in 'economic' investment strategies in leaf construction (Wright *et al.*, 2004), as higher investments in the Andean sites are associated with longer leaf lifespan (Girardin *et al.*, 2014a,b; Huaraca Huasco *et al.*, 2014; Malhi *et al.*, 2014). We find that lowland rainforest sites tightly cluster (**Fig. 8c**) and that TMCF plots have higher and more variable values for both metrics, and there are substantial variations in our estimates depending on the statistical choices made (illustrated). Nevertheless, we find a strong correlation between leaf *n*-alkane concentrations and LMA ($r^2$ = 0.78; $p < 0.05$; **Fig. 7c**), which offers intriguing possibilities to extend theories about drivers of LMA towards understanding controls on *n*-alkane concentrations.

If generalizable, the covariation between LMA and *n*-alkane concentrations (**Fig. 7c**) could be used to predict variations in *n*-alkane concentrations from the many tropical ecosystems with LMA data (Asner and Martin, 2016). However, these predictions would need to be tested given the large variance between individuals observed here, in particular in the highest elevation sites (**Fig. 5**). We caution the observed relationship between *n*-alkane concentration and LMA may not extend beyond angiosperms as plant waxiness varies across phylogeny (Diefendorf *et al.*, 2011). That study found no correlation between wax concentrations on a mass basis and LMA (Diefendorf *et al.*, 2011), based on few species across a wide phylogenetic diversity, and the angiosperms covered a narrow range of LMA compared to that sampled here. Future work could extend studies of leaf wax traits across geographic regions and phylogeny to further understand differences in foliar investment strategies. We note that this elevation transect was fully-forested and we might expect differences in transects with arid climates and sparse high elevation vegetation.

### 4.7. Leaf wax productivity

519 In this study we introduce a new concept of $NPP_{alk}$, and show that in montane sectors between
520 0.6 and 3.7 km, despite a decline in $NPP_{leaf}$ with elevation, alkane productivity increases with
521 elevation from ca. 300 to 3000 g C $ha^{-1}$ $yr^{-1}$ (forest-plot median values, **Table 2, Fig. 8**). In
522 terms of ecosystem net carbon fixation, the higher $NPP_{alk}$ and lower $NPP_{leaf}$ in the TMCF
523 suggests higher leaf wax production while overall leaf production declines, resulting in an
524 increase in the proportion of foliar investment being diverted to leaf wax. The higher
525 proportional investment in leaves in TMCF (**Table 2**), necessarily diverts resources from other
526 growth, such as canopy height (**Table 1**). However, as C and H are not limiting elements for
527 plants, waxes may represent a relatively cheap investment in foliar biomass and defense.

528 Additional research on living plants would ideally expand quantification of leaf wax alkane
529 concentrations and productivity in biomes around the world in order to better assess $NPP_{alk}$ in
530 different ecosystems, to test whether these altitudinal gradients are generally present.
531 More generally these data lead us to consider whether leaf wax production may systematically
532 vary across other landscapes and ecosystems, and other studies of wax concentrations across
533 suggest that this may be the case (Garcin et al., 2014; Diefendorf et al., 2015), although currently
534 this cannot be compared on a unit area basis.

535 **4.8. Geological significance**

536 Although $NPP_{alk}$ is a minor fraction of carbon fixation in the living forest (**Table 1**), we suggest
537 that it may be geologically important. The leaf wax alkane component of biomass is
538 exceptionally recalcitrant compared to other plant biochemicals (e.g. cellulose) that dominate
539 living plant tissues. Only a few recalcitrant compounds, and a very small fraction of living forest
540 biomass have the potential to enter longer term carbon storage in the soils, rivers and ocean
541 sediments offshore (Hedges & Oades, 1997). We therefore propose that $NPP_{alk}$ be more widely

542 estimated, as one of the components of biosynthesis that has the potential to be exported to soils
543 and sediments and sequestered for millions of years (e.g., Tipple and Pagani, 2010).

544 $NPP_{alk}$ also has implications for contemporary and palaeoecological research involving the
545 extraction of leaf wax biomarkers from riverine (Ponton et al., 2014) and marine sediments
546 (Hughen et al., 2004). Higher $NPP_{alk}$ production in montane ecosystems would suggest higher
547 inputs into soils and given lower respiration rates and higher C stocks (Clark et al., 2015), this
548 may be compounded leading to higher carbon stocks in soils. Similarly following erosion of soils
549 into rivers, we might then expect over-representation (on an area basis) of mountain ecosystems
550 in downstream sedimentary records, all else being equal. Higher $NPP_{alk}$ in the TMCF versus the
551 rainforest, together with better preservation in soils at colder temperatures and higher erosive
552 potential from steep, Andean slopes lead us to the hypothesis that tropical montane forests may
553 be disproportionate represented in geological archives in contrast to the more productive but less
554 waxy and more rapidly decomposing waxes from the TR. However, there are many additional
555 steps after leaf wax production that determine the final fate of leaf wax produced by a plant.
556 These steps include 1) decomposition in leaf litter and soils, 2) residence time in soils on the
557 landscape, 3) erosion from soils into rivers, 4) preservation during fluvial transport and 5)
558 preservation upon deposition in sedimentary basins. Some of these steps are sensitive to climate,
559 e.g., greater preservation at the cooler temperatures in higher elevation soils and frequency of
560 mass wasting from Andean slopes (Clark et al., 2015); yet others will depend on the degree of
561 association with inorganic erosion via mineral-organic associations in transit that may offer
562 'packaging' (Kleber et al., 2007). Further discussion of these sedimentary processes are beyond
563 the scope of this living-plant centered manuscript. However, we suggest the possibility of
564 varying plant 'source-strength' identified in this ecosystem, may need to be factored into studies

565 of catchment sourcing to accurately quantify processes of remineralization versus preservation
566 for catchment carbon cycling considerations. Initial comparisons suggest that the greater
567 production of leaf wax compounds in Andean forests does not lead to overrepresentation
568 downstream (Ponton et al., 2014), thus we infer that processes of degradation during fluvial
569 transport (4) must be substantial. Here, our data add to the source end of the source-to-sink
570 journey of leaf wax molecules in a tropical forest transect.

571 **4.9. Future work: other wax components**

572 In this study, we focused on obtaining a very large sample of leaf wax *n*-alkanes and their
573 molecular abundance distribution. While we did not analyze or quantify other wax components
574 in the full sample set, a subset of the samples reported here were analyzed for their *n*-alkanoic
575 acid and *n*-alkane concentrations, as well as the hydrogen isotopic compositions (Feakins et al.,
576 2016). *n*-Alkanoic acid concentrations were found to be much lower than *n*-alkane
577 concentrations in that study (alkane/acid mean 9 ± 3, se). Similarly, a study of North American
578 taxa has shown that *n*-alkanes are among the most abundant compounds found in evergreen
579 angiosperm leaf waxes, representing ~2/3 of waxes, the proportions vary between plant types,
580 with *n*-alkane contributions being much smaller fractions of overall waxes in the deciduous
581 angiosperms and negligible in the gymnosperms (Diefendorf *et al.*, 2011).

582 Regarding plant function of the various wax components, *n*-alkanes are the most hydrophobic of
583 the alkyl lipids due to the non-polar nature of long chain hydrocarbons and may play a key role
584 in water-shedding and defense against cloud forest pressures. It would be valuable to quantify
585 and characterize taxonomic and environmental variations in other wax components, which may
586 play different roles in defense and thus might have different spatial distribution patterns. For
587 example we might terpenoids are involved in insect defense (Giri et al., 2015), and we may

588 hypothesize that these components may decrease with increasing elevation and reduced
589 herbivory pressure.

590 The insights from leaf wax *n*-alkane traits provide a geologically-useful start – these are the
591 components best represented in the molecular fossil record. Although we found ACL had little
592 promise as a palaeothermometer, leaf wax isotopic composition carries important information
593 about hydroclimate (Polissar & Freeman, 2010), and to reconstruct tropical paleoecology and
594 paleoclimate (Schefuss et al., 2003; Schefuss et al., 2005). However other compounds,
595 particularly the *n*-alkanoic acids have been found useful in river catchments (Ponton *et al.*, 2014)
596 and palaeoclimate (Fornace *et al.*, 2014) applications. Further, sedimentary studies have shown
597 differences in compound-classes upon fluvial export (Hemingway et al., 2016). Additional
598 modern plant calibration studies, surveying the other components of wax biochemistry, have the
599 potential to expand our understanding of plant sourcing of sedimentary proxies as well as the
600 tropical forest ecological significance of those wax compositions.

601 **5. Conclusions**

602 In this study we report a large scale study of plant wax *n*-alkane concentrations and molecular
603 abundance distributions in tropical lowland rainforest and TMCF in Peru. Towards higher
604 elevations, plants divert more resources to foliar biomass as a proportion of overall biomass
605 ($NPP_{leaf}$ increases as a proportion of NPP) and within leaf chemistry they divert more of their
606 production to *n*-alkanes. As a result of intensive studies of these forest plots we are able to
607 calculate a new measure of $NPP_{alk}$. These findings are of ecological significance as plant foliar
608 biochemical allocations may represent adaptations to environment as part of investment and
609 defense strategies. Further testing of these concentration patterns in other elevation gradient
610 would allow for testing of the hypothesized links between temperature and other environmental

611 gradients and the robustness of these patterns to ecosystem community change. These findings
612 are of geological significance as these biochemical leave a legacy that remains far beyond the
613 lifetime of the plant, in soils, rivers and ocean sediments, and they offer molecular clues to past
614 forest production. While alkanes are a small fraction of $NPP_{leaf}$ (<0.23%) these compounds
615 survive post-mortem and contribute to long-term C-sequestration in soils and sediments.
616 Connections to studies of leaf wax concentrations in soils and sediments will allow for
617 characterization of how these production changes translate into sedimentary sequestration.

618 **Acknowledgements**

619 Contributing authors are part of the Andes Biodiversity and Ecosystems Research Group ABERG
620 (andesresearch.org), the Global Ecosystems Monitoring (GEM) network (gem.tropicalforests.ox.ac.uk)
621 and the Amazon Forest Inventory Network RAINFOR (www.rainfor.org) research consortia. The field
622 campaign was funded by grants to YM from the UK Natural Environment Research Council (Grants
623 NE/D01025X/1, NE/D014174/1), with additional support from European Research Council (Belgium)
624 advanced investigator grants GEM-TRAITS (321131) and T-FORCES (291585) as well as the Jackson
625 Foundation to YM and a John D. and Catherine T. MacArthur Foundation grant to GA. GA and the
626 spectranomics team were supported by the endowment of the Carnegie Institution for Science, and by the
627 US National Science Foundation (DEB-1146206), supporting the taxonomic contributions to the
628 project. Carnegie Airborne Observatory data collection, processing and analyses were funded solely by
629 the John D. and Catherine T. MacArthur Foundation. The Carnegie Airborne Observatory is supported by
630 the Avatar Alliance Foundation, John D. and Catherine T. MacArthur Foundation, Andrew Mellon
631 Foundation, David and Lucile Packard Foundation, Mary Anne Nyburg Baker and G. Leonard Baker Jr.,
632 and William R. Hearst III (all USA). Laboratory work at USC was in part supported by the US National
633 Science Foundation (EAR-1227192) and the ACS Petroleum Research Fund (53747-ND2) to SF. In Peru,
634 we thank the Servicio Nacional de Áreas Naturales Protegidas por el Estado (SERNANP) and personnel

635 of Manu and Tambopata National Parks for logistical assistance and permission to work in the protected
636 areas. We also thank the Explorers' Inn and the Pontifical Catholic University of Peru (PUCP), as well as
637 Amazon Conservation Association for use of the Tambopata and Wayqecha Research Stations,
638 respectively. Many researchers were involved in the field, in particular we would like to thank E. Cosio,
639 W. Huaraca-Huasca and J. Huaman for advising on field logistics; tree climbers: C. Costas, D. Chacón,
640 H. Ninatay; field project supervision: T. Boza, M. Raurau; species identification and basal area: W.
641 Farfan, F. Sinca; leaf areas R.M. Castro, G. Rayme, A. Robles, Y. Choque and Y. Valdez. We thank USC
642 undergraduate Jeremy Sunwoo for laboratory assistance. This manuscript was improved with the
643 comments of 3 anonymous reviewers.

## 644 APPENDIX A. SUPPLEMENTARY DATA

645 Supplementary data associated with this article can be found, in the online version, at
646 http://dx.doi.org/10..... The data include interactive Google Earth maps of the sampling locations
647 described in this article.

## 648 References

649 Asner, G.P., Anderson, C.B., Martin, R.E., Knapp, D.E., Tupayachi, R., Sinca, F. and Malhi, Y.
650 (2014a) Landscape-scale changes in forest structure and functional traits along an Andes-
651 to-Amazon elevation gradient. Biogeosciences 11, 843–856.
652 Asner, G.P., Llactayo, W., Tupayachi, R. and Luna, E.R. (2013) Elevated rates of gold mining in
653 the Amazon revealed through high-resolution monitoring. Proceedings of the National
654 Academy of Sciences, doi: 10.1073/pnas.1318271110.
655 Asner, G.P., Martin, R.E., Carranza-Jimenez, L., Sinca, F., Tupayachi, R., Anderson, C.B. and
656 Martinez, P. (2014b) Functional and biological diversity of foliar spectra in tree canopies
657 throughout the Andes to Amazon region. New Phytologist 204, 127–139.
658 Asner, G.P. and Martin, R.E. (2016) Convergent elevation trends in canopy chemical traits of
659 tropical forests. Global Change Biology, doi: 10.1111/gcb.13164.
660 Baker, P.A., Fritz, S.C., Silva, C.G., Rigsby, C.A., Absy, M.L., Almeida, R.P., Caputo, M.,
661 Chiessi, C.M., Cruz, F.W., Dick, C.W., Feakins, S.J., Figueiredo, J., Freeman, K.H.,
662 Hoorn, C., Jaramillo, C., Kern, A.K., Latrubesse, E.M., Ledru, M.P., Marzoli, A., Myrbo,
663 A., Noren, A., Piller, W.E., Ramos, M.I.F., Ribas, C.C., Trnadade, R., West, A.J.,
664 Wahnfried, I. and Willard, D.A. (2015) Trans-Amazon Drilling Project (TADP): origins
665 and evolution of the forests, climate, and hydrology of the South American tropics.
666 Scientific Drilling 20, 41–49.
667 Bingham, E.M., McClymont, E.L., Valiranta, M., Mauquoy, D., Roberts, Z., Chambers, F.M.,
668 Pancost, R.D. and Evershed, R.P. (2010) Conservative composition of n-alkane

669 biomarkers in Sphagnum species: implications for palaeoclimate reconstruction in
670 ombrotrophic peat bogs. Organic Geochemistry 41, 214–220.
671 Bush, R.T. and McInerney, F.A. (2013) Leaf wax n-alkane distributions in and across modern
672 plants: Implications for paleoecology and chemotaxonomy. Geochimica et
673 Cosmochimica Acta in press.
674 Carr, A.S., Boom, A. and Chase, B.M. (2010) The potential of plant biomarker evidence derived
675 from rock hyrax middens as an indicator of palaeoenvironmental change. Paleogeography
676 Paleoclimatology Paleoecology 285, 321–330.
677 Castaneda, I.S., Mulitza, S., Schefuss, E., Lopes dos Santos, R.A., Sinninghe Damste, J.S. and
678 Schouten, S. (2009) Wet phases in the Sahara/Sahel region and human migration patterns
679 in North Africa. Proceedings of the National Academy of Sciences 106, 20159–20163.
680 Clark, K.E., West, A.J., Hilton, R.G., Asner, G.P., Quesada, C.A., Silman, M.R., Saatchi, S.S.,
681 Farfan-Rios, W., Martin, R.E., Horwath, A.B., Halladay, K., New, M. and Malhi, Y.
682 (2015) Storm-triggered landslides in the Peruvian Andes and implications for
683 topography, carbon cycles, and biodiversity. Earth Surf. Dynam. Discuss. 3, 631–688.
684 Condit, R., Pitman, N., Leigh, E.G., Chave, J., Terborgh, J., Foster, R.B., Nunez, P., Aguilar, S.,
685 Valencia, R., Villa, G., Muller-Landau, H.C., Losos, E. and Hubbell, S.P. (2002) Beta-
686 diversity in tropical forest trees. Science 295, 666-669.
687 Diefendorf, A.F., Freeman, K.H., Wing, S.L. and Graham, H.V. (2011) Production of n-alkyl
688 lipids in living plants and implications for the geologic past. Geochimica et
689 Cosmochimica Acta 75, 7472–7485.
690 Diefendorf, A.F., Leslie, A.B. and Wing, S.L. (2015) Leaf wax composition and carbon isotopes
691 vary among major conifer groups. Geochimica Et Cosmochimica Acta 170, 145-156.
692 Eglinton, G., Gonzalez, A.G., Hamilton, R.J. and Raphael, R.A. (1962) Hydrocarbon
693 constituents of the wax coatings of plant leaves: A taxonomic survey. Phytochemistry 1,
694 89–102.
695 Eglinton, G. and Hamilton, R.J. (1963) CHAPTER 8 - The Distribution of Alkanes A2 -
696 SWAIN, T, Chemical Plant Taxonomy. Academic Press, pp. 187–217.
697 Eglinton, G. and Hamilton, R.J. (1967) Leaf epicuticular waxes. Science 156, 1322–1335.
698 Feakins, S.J., Bentley, L.P., Salinas, N., Shenkin, A., Blonder, B., Goldsmith, G.R., Ponton, C.,
699 Arvin, L.J., Wu, M.S., Peters, T., West, A.J., Martin, R.E., Enquist, B.J., Asner, G.P. and
700 Malhi, Y. (2016) Plant leaf wax biomarkers capture gradients in hydrogen isotopes of
701 precipitation from the Andes and Amazon. Geochimica et Cosmochimica Acta 182, 155–
702 172.
703 Fornace, K.L., Hughen, K.A., Shanahan, T.M., Fritz, S.C., Baker, P.A. and Sylva, S.P. (2014) A
704 60,000-year record of hydrologic variability in the Central Andes from the hydrogen
705 isotopic composition of leaf waxes in Lake Titicaca sediments. Earth and Planetary
706 Science Letters 408, 263–271.
707 Garcin, Y., Schefuß, E., Schwab, V.F., Garreta, V., Gleixner, G., Vincens, A., Todou, G., Séné,
708 O., Onana, J.-M., Achoundong, G. and Sachse, D. (2014) Reconstructing C3 and C4
709 vegetation cover using *n*-alkane carbon isotope ratios in recent lake sediments from
710 Cameroon, Western Central Africa. Geochimica et Cosmochimica Acta 142, 482–500.
711 Girardin, C.A.J., Espejob, J.E.S., Doughty, C.E., Huasco, W.H., Metcalfe, D.B., Durand-Baca,
712 L., Marthews, T.R., Aragao, L., Farfan-Rios, W., Garcia-Cabrera, K., Halladay, K.,
713 Fisher, J.B., Galiano-Cabrera, D.F., Huaraca-Quispe, L.P., Alzamora-Taype, I., Eguiluz-
714 Mora, L., Salinas-Revilla, N., Silman, M.R., Meir, P. and Malhi, Y. (2014a) Productivity

715 and carbon allocation in a tropical montane cloud forest in the Peruvian Andes. Plant
716 Ecology & Diversity 7, 107–123.
717 Girardin, C.A.J., Farfan-Rios, W., Garcia, K., Feeley, K.J., Jorgensen, P.M., Murakami, A.A.,
718 Perez, L.C., Seidel, R., Paniagua, N., Claros, A.F.F., Maldonado, C., Silman, M., Salinas,
719 N., Reynel, C., Neill, D.A., Serrano, M., Caballero, C.J., Cuadros, M.D.L., Macia, M.J.,
720 Killeen, T.J. and Malhi, Y. (2014b) Spatial patterns of above-ground structure, biomass
721 and composition in a network of six Andean elevation transects. Plant Ecology &
722 Diversity 7, 161–171.
723 Giri, S.J., Diefendorf, A.F. and Lowell, T.V. (2015) Origin and sedimentary fate of plant-derived
724 terpenoids in a small river catchment and implications for terpenoids as quantitative
725 paleovegetation proxies. Organic Geochemistry 82, 22–32.
726 Graham, H.V., Patzkowsky, M.E., Wing, S.L., Parker, G.G., Fogel, M.L. and Freeman, K.H.
727 (2014) Isotopic characteristics of canopies in simulated leaf assemblages. Geochimica et
728 Cosmochimica Acta 144, 82–95.
729 Handley, L., O'Halloran, A., Pearson, P.N., Hawkins, E., Nicholas, C.J., Schouten, S., McMillan,
730 I.K. and Pancost, R.D. (2012) Changes in the hydrological cycle in tropical East Africa
731 during the Paleocene-Eocene Thermal Maximum. Paleogeography Paleoclimatology
732 Paleoecology 329, 10–21.
733 Hedges, J.I. and Oades, J.M. (1997) Comparative organic geochemistries of soils and marine
734 sediments. Organic Geochemistry 27, 319–361.
735 Hemingway, J.D., Schefuß, E., Dinga, B.J., Pryer, H. and Galy, V.V. (2016) Multiple plant-wax
736 compounds record differential sources and ecosystem structure in large river catchments.
737 Geochimica et Cosmochimica Acta 184, 20–40.
738 Hoffmann, B., Kahmen, A., Cernusak, L.A., Arndt, S.K. and Sachse, D. (2013) Abundance and
739 distribution of leaf wax *n*-alkanes in leaves of Acacia and Eucalyptus trees along a strong
740 humidity gradient in northern Australia. Organic Geochemistry 62, 62–67.
741 Hoorn, C., Wesselingh, F.P., ter Steege, H., Bermudez, M.A., Mora, A., Sevink, J., Sanmartin, I.,
742 Sanchez-Meseguer, A., Anderson, C.L., Figueiredo, J.P., Jaramillo, C., Riff, D., Negri,
743 F.R., Hooghiemstra, H., Lundberg, J., Stadler, T., Sarkinen, T. and Antonelli, A. (2010)
744 Amazonia Through Time: Andean Uplift, Climate Change, Landscape Evolution, and
745 Biodiversity. Science 330, 927–931.
746 Huacara Huasco, W., Girardin, C.A.J., Doughty, C.E., Metcalfe, D.B., Baca, L.D., Silva-Espejo,
747 J.E., Cabrera, D.G., Aragao, L., Davila, A.R., Marthews, T.R., Huaraca-Quispe, L.P.,
748 Alzamora-Taype, I., Mora, L.E., Farfan-Rios, W., Cabrera, K.G., Halladay, K., Salinas-
749 Revilla, N., Silman, M.R., Meir, P. and Malhi, Y. (2014) Seasonal production, allocation
750 and cycling of carbon in two mid-elevation tropical montane forest plots in the Peruvian
751 Andes. Plant Ecology & Diversity 7, 125–142.
752 Hughen, K., Eglinton, T., Xu, L. and Makou, M. (2004) Abrupt tropical vegetation response to
753 rapid climate changes. Science 304, 1955–1959.
754 Jansen, B., de Boer, E.J., Cleef, A.M., Hooghiemstra, H., Moscol-Olivera, M., Tonneijck, F.H.
755 and Verstraten, J.M. (2013) Reconstruction of late Holocene forest dynamics in northern
756 Ecuador from biomarkers and pollen in soil cores. Paleogeography Paleoclimatology
757 Paleoecology 386, 607–619.
758 Jansen, B., Haussmann, N.S., Tonneijck, F.H., Verstraten, J.M. and de Voogt, P. (2008)
759 Characteristic straight-chain lipid ratios as a quick method to assess past forest-paramo
760 transitions in the Ecuadorian Andes. Paleogeogr. Paleoclimatol. Paleoecol. 262, 129–139.

761 Jansen, B. and Nierop, K.G.J. (2009) Methyl ketones in high altitude Ecuadorian Andosols
762 confirm excellent conservation of plant-specific *n*-alkane patterns. Organic Geochemistry
763 40, 61–69.
764 Jansen, B., Nierop, K.G.J., Hageman, J.A., Cleef, A.M. and Verstraten, J.M. (2006) The straight-
765 chain lipid biomarker composition of plant species responsible for the dominant biomass
766 production along two altitudinal transects in the Ecuadorian Andes. Organic
767 Geochemistry 37, 1514–1536.
768 Jansen, B., van Loon, E.E., Hooghiemstra, H. and Verstraten, J.M. (2010) Improved
769 reconstruction of palaeo-environments through unravelling of preserved vegetation
770 biomarker patterns. Paleogeography Paleoclimatology Paleoecology 285, 119–130.
771 Jetter, R. and Schaffer, S. (2001) Chemical composition of the Prunus laurocerasus leaf surface.
772 Dynamic changes of the epicuticular wax film during leaf development. Plant Physiology
773 126, 1725–1737.
774 Kahmen, A., Schefuss, E. and Sachse, D. (2013a) Leaf water deuterium enrichment shapes leaf
775 wax n-alkane delta D values of angiosperm plants I: Experimental evidence and
776 mechanistic insights. Geochimica Et Cosmochimica Acta 111, 39–49.
777 Kawamura, K., Ishimura, Y. and Yamazaki, K. (2003) Four years' observations of terrestrial
778 lipid class compounds in marine aerosols from the western North Pacific. Global
779 Biogeochemical Cycles 17, 1003, doi:10.1029/2001GB001810.
780 Kleber, M., Sollins, P. and Sutton, R. (2007) A conceptual model of organo-mineral interactions
781 in soils: self-assembly of organic molecular fragments into zonal structures on mineral
782 surfaces. Biogeochemistry 85, 9–24.
783 Koch, K., Bhushan, B. and Barthlott, W. (2009) Multifunctional surface structures of plants: An
784 inspiration for biomimetics. Progress in Materials Science 54, 137–178.
785 Krishnan, S., Pagani, M. and Agnini, C. (2015) Leaf waxes as recorders of paleoclimatic changes
786 during the Paleocene-Eocene Thermal Maximum: Regional expressions from the Belluno
787 Basin. Organic Geochemistry 80, 8–17.
788 Malhi, Y., Amezquita, F.F., Doughty, C.E., Silva-Espejo, J.E., Girardin, C.A.J., Metcalfe, D.B.,
789 Aragao, L., Huaraca-Quispe, L.P., Alzamora-Taype, I., Eguiluz-Mora, L., Marthews,
790 T.R., Halladay, K., Quesada, C.A., Robertson, A.L., Fisher, J.B., Zaragoza-Castells, J.,
791 Rojas-Villagra, C.M., Pelaez-Tapia, Y., Salinas, N., Meir, P. and Phillips, O.L. (2014)
792 The productivity, metabolism and carbon cycle of two lowland tropical forest plots in
793 south-western Amazonia, Peru. Plant Ecology & Diversity 7, 85–105.
794 Malhi, Y., Silman, M., Salinas, N., Bush, M., Meir, P. and Saatchi, S. (2010) Introduction:
795 Elevation gradients in the tropics: laboratories for ecosystem ecology and global change
796 research. Global Change Biology 16, 3171–3175.
797 Metcalfe, D.B., Asner, G.P., Martin, R.E., Silva Espejo, J.E., Huasco, W.H., Farfán Amézquita,
798 F.F., Carranza-Jimenez, L., Galiano Cabrera, D.F., Baca, L.D., Sinca, F., Huaraca
799 Quispe, L.P., Taype, I.A., Mora, L.E., Dávila, A.R., Solórzano, M.M., Puma Vilca, B.L.,
800 Laupa Román, J.M., Guerra Bustios, P.C., Revilla, N.S., Tupayachi, R., Girardin, C.A.J.,
801 Doughty, C.E. and Malhi, Y. (2014) Herbivory makes major contributions to ecosystem
802 carbon and nutrient cycling in tropical forests. Ecology Letters 17, 324–332.
803 Noble, D.C., McKee, E.H. and Megard, F. (1979) Early Tertiary “Incaic” tectonism, uplift, and
804 volcanic activity, Andes of central Peru. Geol. Soc. Am. Bull. 90, 903–907.

Pagani, M., Pedentchouk, N., Huber, M., Sluijs, A., Schouten, S., Brinkhuis, H., Damste, J.S.S. and Dickens, G.R. (2006) Arctic hydrology during global warming at the Palaeocene/Eocene thermal maximum. Nature 442, 671–675.

Paine, C.E.T., Baraloto, C. and Díaz, S. (2015) Optimal strategies for sampling functional traits in species-rich forests. Functional Ecology 29, 1325–1331.

Pearson, A. and Eglinton, T. (2000) The origin of *n*-alkanes in Santa Monica Basin surface sediment: a model based on compound-specific Δ14C and $\delta^{13}C$ data. Organic Geochemistry 31, 1103–1116.

Polissar, P.J. and Freeman, K.H. (2010) Effects of aridity and vegetation on plant-wax [delta]D in modern lake sediments. Geochimica et Cosmochimica Acta 74, 5785–5797.

Ponton, C., West, A.J., Feakins, S.J. and Galy, V. (2014) Leaf wax biomarkers in transit record river catchment composition. Geophysical Research Letters 41, 6420–6427.

Reuter, H.I., Nelson, A. and Jarvis, A. (2007) An evaluation of void filling interpolation methods for SRTM data, International Journal of Geographic Information Science. 21, 983–1008.

Schefuss, E., Schouten, S., Jansen, J.H.F. and Damste, J.S.S. (2003) African vegetation controlled by tropical sea surface temperatures in the mid-Pleistocene period. Nature 422, 418–421.

Schefuss, E., Schouten, S. and Schneider, R. (2005) Climatic controls on central African hydrology during the past 20,000 years. Nature 473, 1003–1006.

Silman, M.R. (2014) Functional megadiversity. Proceedings of the National Academy of Sciences 111, 5763–5764.

Tipple, B.J., Berke, M.A., Doman, C.E., Khachaturyan, S. and Ehleringer, J.R. (2013) Leaf-wax n-alkanes record the plant–water environment at leaf flush. Proceedings of the National Academy of Sciences 110, 2659–2664.

Tipple, B.J. and Pagani, M. (2013) Environmental control on eastern broadleaf forest species' leaf wax distributions and D/H ratios. Geochimica et Cosmochimica Acta 111, 64-77.

Vogts, A., Moossen, H., Rommerskirchen, F. and Rullkotter, J. (2009) Distribution patterns and stable carbon isotopic composition of alkanes and alkan-1-ols from plant waxes of African rain forest and savanna C-3 species. Organic Geochemistry 40, 1037–1054.

837

838 **Figure Legends**

839 **Fig. 1:** Location of 9 CHAMBASA forest plots on an elevation transect across the eastern slope
840 of the Andes in southern Peru. Site locations (open circles, site name annotated), vegetation
841 zones, cloud base and river proximity indicated. Elevation profile: grey line (elevation acquired
842 from the Shuttle Radar Topographic Mission (SRTM) 90m Digital Elevation Database 4.1
843 (Reuter et al., 2007), black line (smoothed elevation), grey envelope (topography; ±2σ elevation
844 from 1km-wide swath perpendicular to transect, re-centered to smoothed elevation). R code
845 available from https://gist.github.com/ashenkin/7fceb77e78efc33961a8. For interactive map of
846 study locations see Appendix A.

847

848 **Fig. 2:** *n*-Alkane molecular abundance distribution. Showing the relative molecular abundance
849 distribution of all individuals (n = 552) across all 9 sites. Variability not shown, see Appendix A.

850

851 **Fig. 3:** Molecular abundance indices for individual data (black +; n = 552) **a)** $C_{29}/C_{31}$ and **b)** CPI.

852

853 **Fig. 4:** Average Chain Length (ACL) showing species means at each site (blue circles; n = 152)
854 overlain on individual data (black dot; n = 552) with unweighted site mean values (black dash
855 symbol; n = 9) and linear regression of site mean values (thick black line), see text.

856

857 **Fig. 5:** Total alkane concentration **a)** per gram dry leaf, **a)** per gram dry leaf on C basis and **c)**
858 per unit area. Showing data for individuals (+).

859

**Fig. 6: a)** Total alkane concentration per unit area, showing individuals (black dots), species averages (blue circles) and community weighted mean (green dasb symbol). **b)** Violin plot (zoomed in) showing the distribution of individual data (using a Gaussian kernel density function), the median (red line), the mean (thick black line). Also showing community representation: fraction of basal area represented by sampling (pie charts), with number of individuals and species sampled.

**Fig. 7: a)** Leaf mass per area (LMA) for forest plots, **b)** total alkane concentration per leaf area and **c)** LMA versus Σalk. Showing median (red triangles), mean (black squares) and standard error of the mean (error bars), and community-weighted mean (cmw; green squares) and weighted standard error (error bars). Data cluster (demarcated by dashed lines) for the tropical lowland rainforest, as distinct from the Tropical Montane Cloud Forest which has higher values and greater variability (note y axis break). Regression is shown for the plot mean values only (black line), $y = 0.14x - 12$ ($R^2 = 0.78$, $p < 0.05$).

**Fig. 8: a)** Total alkane concentration on a carbon basis, showing median (red triangles), mean (black squares) showing standard error of the mean (error bars), and community-weighted mean values (green squares), showing weighted standard error of the mean (error bars). **b)** $NPP_{leaf}$ for each forest plot, showing standard errors (error bars) and linear regression $y = -0.53x - 3.9$ ($R^2 = 0.67$, $p < 0.05$) (Girardin *et al.*, 2014a; Huaraca Huasco *et al.*, 2014; Malhi *et al.*, 2014; and this study), **c)** $NPP_{alk}$ for each forest plot, symbols as in a).

881 **Table 1** Environmental and ecological characteristics of 1 ha forest plots along a tropical montane elevation transect.

| CHAMBASA/ RAINFOR site | TAM-06 | TAM-05 | PAN-02 | PAN-03 | SPD-02 | SPD-01 | TRU-04 | ESP-01 | ACJ-01 |
|---|---|---|---|---|---|---|---|---|---|
| Latitude | −12.8385 | −12.8309 | −12.6495 | −12.6383 | −13.0491 | −13.0475 | −13.1055 | −13.1751 | −13.14689 |
| Longitude | −69.2960 | −69.2705 | −71.2626 | −71.2744 | −71.5365 | −71.5423 | −71.5893 | −71.5948 | −71.6323 |
| Elevation* (m) | 215 | 223 | 595 | 859 | 1494 | 1713 | 2719 | 2868 | 3537 |
| Slope* (deg) | 2.2 | 4.5 | 11.5 | 13.7 | 27.1 | 30.5 | 21.2 | 27.3 | 36.3 |
| Aspect* (deg) | 169 | 186 | 138 | 160.5 | 125 | 117 | 118 | 302 | 104 |
| MAAT.** (°C) | 24.4 | 24.4 | 23.5** | 21.9** | 18.8 | 17.4 | 13.5 | 13.1 | 9 |
| Precipitation (mm $yr^{-1}$) | 1900 | 1900 | 2366** | 2835** | 5302 | 5302 | 2318 | 1560 | 1980 |
| Vegetation height* | 28.2 | 27.5 | 24.4 | 18.7 | 22.8 | 14.0 | 15.7 | 16.9 | 12.5 |

882 *Derived from high-resolution airborne Light Detection and Ranging (LiDAR) data (see Asner et al., 2013 for methodology). **MAAT = mean annual air
883 temperature, derived from observations between 6 Feb 2013 and 7 Jan 2014.

884

885 **Table 2** Leaf waxes as a component of net primary productivity

| | | Alkane concentration (μg $g^{-1}$ C) | | | | | NPP (Mg $Cha^{-1}$ $yr^{-1}$) | | | | $NPP_{alk}$ (g C $ha^{-1}$ $yr^{-1}$) | | | | | md $NPP_{alk}$ (%) | |
|---|---|---|---|---|---|---|---|---|---|---|---|---|---|---|---|---|---|
| Site | Elev. (km) | md | me | se | cwm | wse | NPP | se | $NPP_{leaf}$ | se | md | me | c.se | cwm | c.wse | of $NPP_{leaf}$ | of NPP |
| TAM-06 | 0.215 | 185 | 323 | 42 | 170 | 42 | 12 | 0.6 | 3.7 | 0.4 | 686 | 1199 | 42 | 631 | 31 | 0.02 | 0.006 |
| TAM-05 | 0.223 | 272 | 375 | 42 | 364 | 42 | 15 | 0.8 | 4.0 | 0.3 | 1098 | 1513 | 42 | 1466 | 32 | 0.03 | 0.007 |
| PAN-02 | 0.595 | 96 | 191 | 32 | 267 | 32 | 11 | 0.7 | 3.5 | 0.1 | 340 | 676 | 32 | 944 | 25 | 0.01 | 0.003 |
| PAN-03 | 0.859 | 106 | 182 | 61 | 196 | 61 | 9 | 0.6 | 3.0 | 0.1 | 321 | 552 | 61 | 595 | 39 | 0.01 | 0.003 |
| SPD-02 | 1.494 | 108 | 309 | 54 | 386 | 54 | 13 | 0.5 | 4.1 | 0.2 | 446 | 1272 | 54 | 1590 | 40 | 0.01 | 0.004 |
| SPD-01 | 1.713 | 452 | 649 | 69 | 678 | 69 | 8 | 0.4 | 2.6 | 0.2 | 1188 | 1706 | 69 | 1783 | 42 | 0.05 | 0.014 |
| TRU-04 | 2.719 | 1126 | 1262 | 156 | 949 | 156 | 8 | 0.4 | 2.7 | 0.0 | 3029 | 3394 | 156 | 2553 | 91 | 0.11 | 0.037 |
| ESP-01 | 2.868 | 834 | 1250 | 186 | 1114 | 186 | 8 | 0.4 | 2.0 | 0.2 | 1635 | 2449 | 186 | 2184 | 160 | 0.08 | 0.021 |
| ACJ-01 | 3.537 | 233 | 1096 | 266 | 2327 | 266 | 8 | 0.5 | 2.2 | 0.1 | 513 | 2413 | 266 | 5123 | 255 | 0.02 | 0.006 |
| min. | 0 | 96 | 182 | | 170 | | 8 | | 2.0 | | 321 | 552 | | 595 | | 0.01 | 0.003 |
| max. | 4 | 1126 | 1262 | | 2327 | | 15 | | 4.1 | | 3029 | 3394 | | 5123 | | 0.11 | 0.037 |

md = median, me = mean, cwm = community-weighted mean, se = standard error, wse = weighted standard error, c. wse. = compound standard error of the mean, calculated as sum of squares of wse for alkane concentration and $NPP_{leaf}$. Site median $NPP_{alk}$ estimate is also reported as a proportion of forest $NPP_{leaf}$ and NPP, alkane production is <<1% because leaf waxes are a small component of forest biomass.

886
887

**Figure 1**

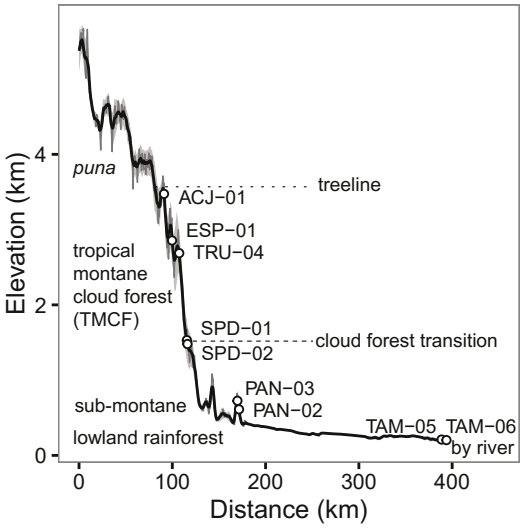
Elevation (km)
4
2
0
0
100
200
300
400
Distance (km)
puna
treeline
ACJ−01
ESP−01
TRU−04
tropical
montane
cloud forest
(TMCF)
SPD−01
cloud forest transition
SPD−02
PAN−03
PAN−02
sub-montane
lowland rainforest
TAM−05 TAM−06
by river

**Figure 2**

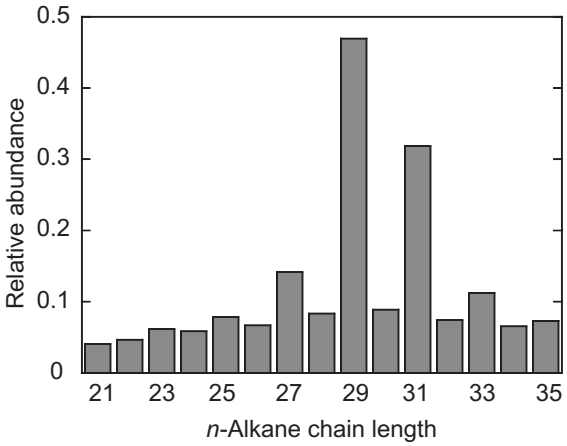
0.5
0.4
0.3
0.2
0.1
0
Relative abundance
21
23
25
27
29
31
33
35
*n*-Alkane chain length

**Figure 3**

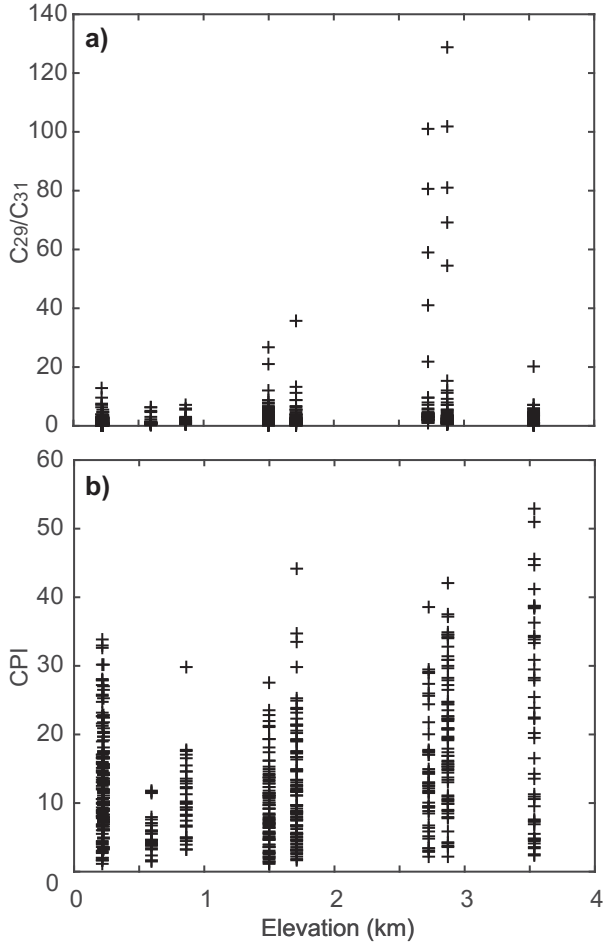
a)
b)
$C_{29}/C_{31}$
CPI
Elevation (km)
0
20
40
60
80
100
120
140
10
30
50
1
2
3
4

**Figure 4**

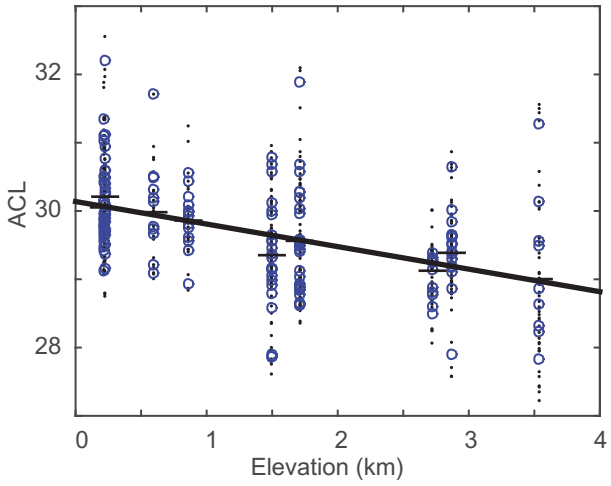

**Figure 5**

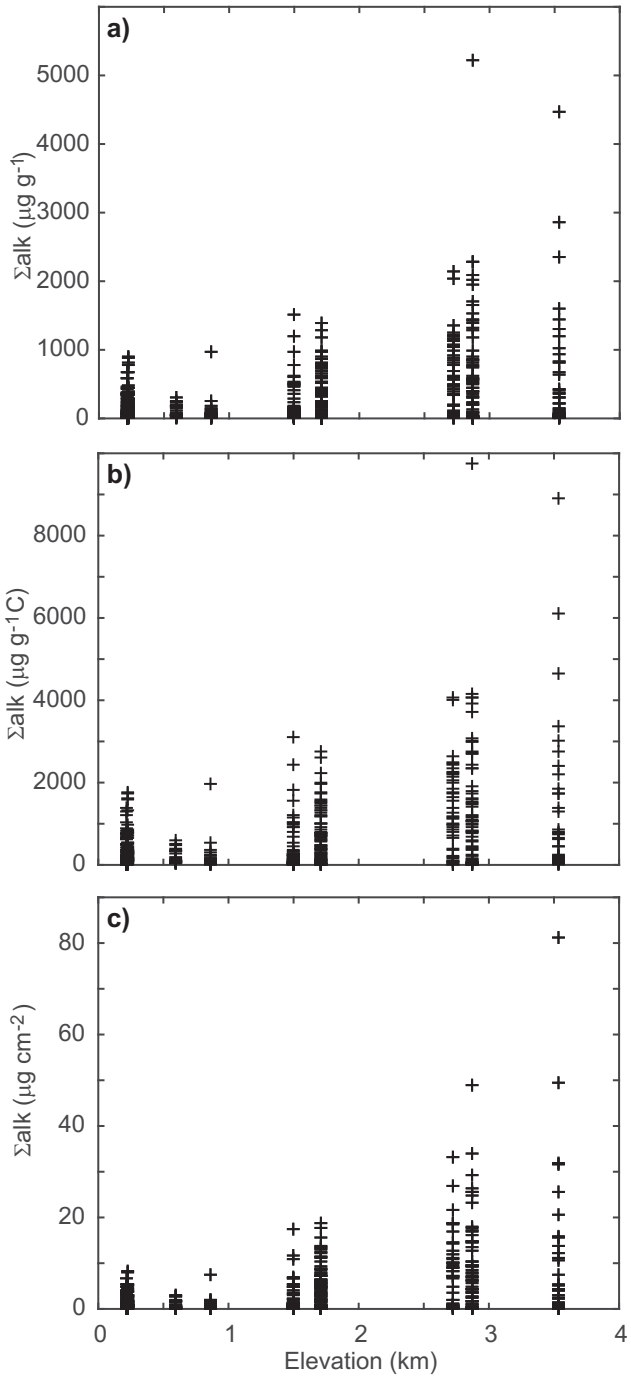
a)
b)
c)
Σalk (μg g-1)
Σalk (μg g-1C)
Σalk (μg cm-2)
Elevation (km)
0
1000
2000
3000
4000
5000
6000
8000
20
40
60
80
1
2
3
4

**Figure 6**

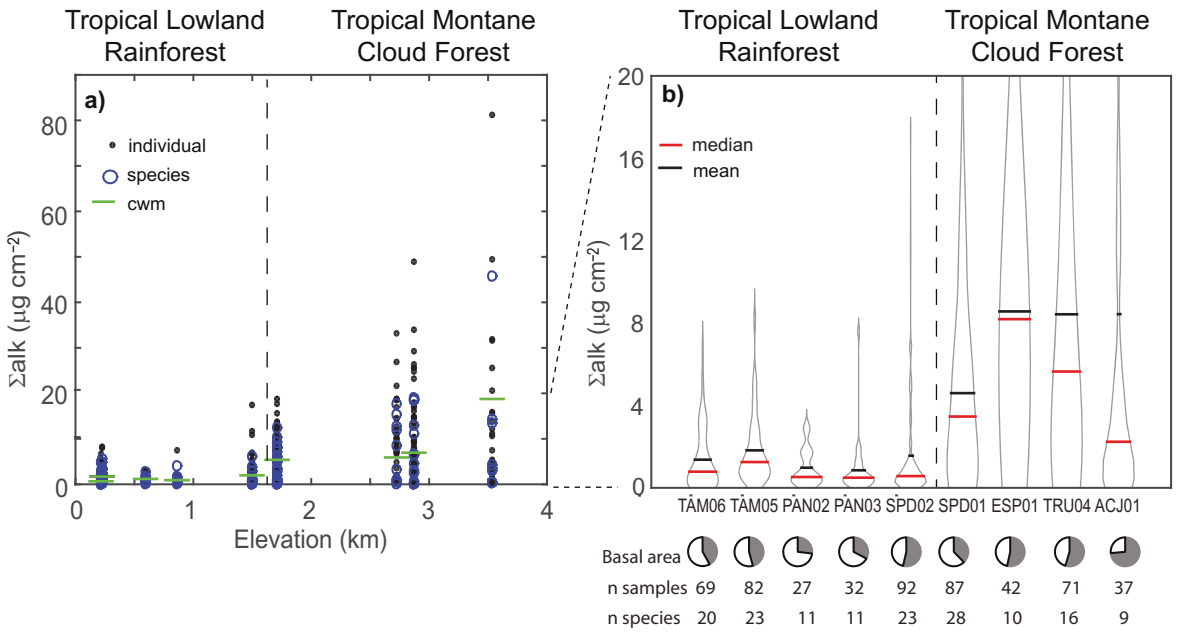
Tropical Lowland Rainforest
Tropical Montane Cloud Forest
a)
individual
species
cwm
Σalk (µg cm-2)
Elevation (km)
b)
median
mean
TAM06 TAM05 PAN02 PAN03 SPD02 SPD01 ESP01 TRU04 ACJ01
Basal area
n samples 69 82 27 32 92 87 42 71 37
n species 20 23 11 11 23 28 10 16 9

**Figure 7**

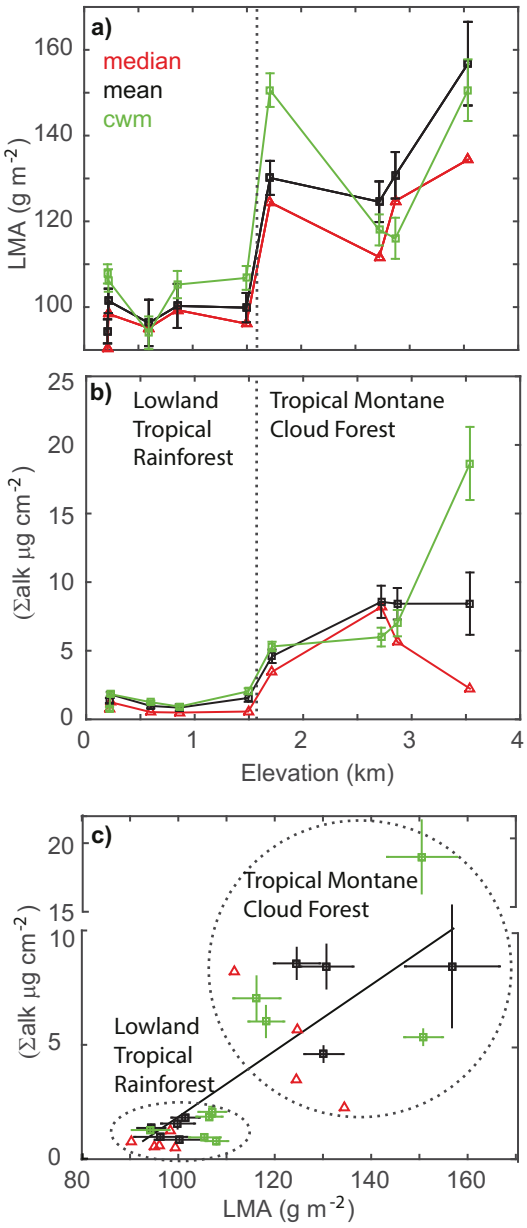
a)
median
mean
cwm
LMA (g m-2)
160
140
120
100
b)
Lowland
Tropical
Rainforest
Tropical Montane
Cloud Forest
(Σalk µg cm-2)
25
20
15
10
5
0
0
1
2
3
4
Elevation (km)
c)
Tropical Montane
Cloud Forest
Lowland
Tropical
Rainforest
(Σalk µg cm-2)
20
15
10
5
0
80
100
120
140
160
LMA (g m-2)

**Figure 8**

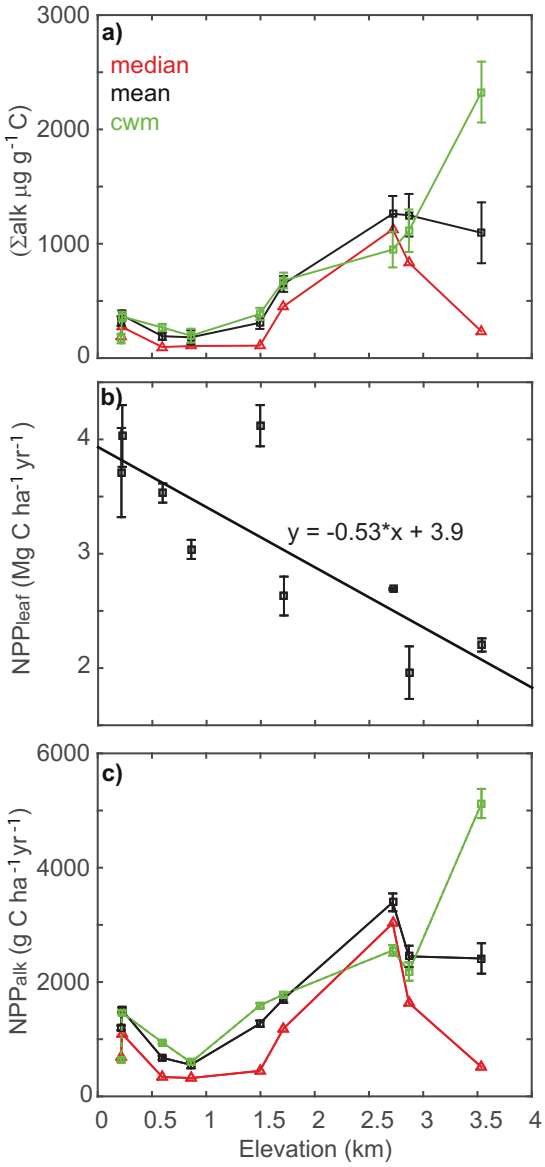
a)
median
mean
cwm
(Σalk µg g-1 C)
3000
2000
1000
0
b)
y = -0.53*x + 3.9
NPPleaf (Mg C ha-1 yr-1)
4
3
2
c)
NPPalk (g C ha-1 yr-1)
6000
4000
2000
0
0
0.5
1
1.5
2
2.5
3
3.5
4
Elevation (km)

**Supplementary Material**

Click here to download Supplementary Material: Appendix A_alkanes.xls

**Interactive Map file (.kml or .kmz)**

**Click here to download Interactive Map file (.kml or .kmz): PeruPlantSites_all.kml**